Geographically Opposing Responses of Sea Urchin Recruitment to Changes in Ocean Climate

Daniel K. Okamoto*[1,2], Daniel C. Reed†[3], and Stephen Schroeter‡[3]

[1]Department of Biological Science, Florida State University, Tallahassee, Florida 32303
[3]Ecology, Evolution and Marine Biology, University of California Santa Barbara, Santa Barbara, CA 93106 USA
[3]Marine Science Institute, University of California Santa Barbara, Santa Barbara, CA 93106 USA

Corresponding Author
Daniel K Okamoto
Department of Biological Science
The Florida State University
Tallahassee, Florida 32303
Phone: (850) 645-9532
emaildokamoto@bio.fsu.edu

Author contributions
DKO, SS, and DR designed research. DKO designed, built and conducted analyses and wrote the initial manuscript. DKO, DCR and SS managed data. SS initiated and oversaw data collection and collaborated on all analyses. All authors contributed to revisions.

*corresponding author: dokamoto@bio.fsu.edu
†email: dan.reed@lifesci.ucsb.edu
‡email: schroete@lifesci.ucsb.edu

Abstract

Sea urchins are voracious herbivores that influence the ecological structure and function of nearshore ecosystems throughout the world. Urchin population growth rates may be particularly sensitive to climate change because adult reproduction and larval development can vary greatly with food availability and temperature, and the transport of their larvae, which spend months feeding in the plankton, are affected by changes in ocean currents. Yet how climate alters sea urchin populations in space and time by modifying larval recruitment and year-class strength remains untested. Using an unprecedented spatially replicated 27-year dataset we illustrate how ocean temperature and climate oscillations differentially affect larval recruitment of the purple sea urchin (*Strongylocentrotus purpuratus*) and give rise to geographic asynchrony between northern California (positive) vs southern California (negative). Importantly, we found a strong correlation between larval recruitment and regional year class strength suggesting that recruitment variation plays an important role in controlling population dynamics. These results are the first to show that climatic fluctuations shape broad-scale patterns of sea urchin larval recruitment and are likely to control dynamics of both populations and marine ecosystems that vary over the geographical range of their distribution.

Introduction

Climate forecasts project large changes in ocean temperature, biogeochemistry and the nature and frequency of disruptive events that affect ocean circulation and primary productivity (e.g. Cai *et al.* 2014; Yeh *et al.* 2009). Such shifts are expected to impose wide-reaching ecological impacts, in part by altering animal recruitment in space and time (Sydeman *et al.* 2015). As a result, characterizing how climate shapes variability in recruitment can provide substantial benefits to the conservation and management of marine resources. For species with planktonic larvae, significant challenges remain in achieving such objectives due to the substantial effort needed to characterize spatial and temporal variation in larval abundance and the numerous sensitive vital rates that contribute to it.

For species like sea urchins, understanding causes and consequences of recruitment variability has both ecological and economic implications. Sea urchin grazing can alter the structure of some of the world's most diverse and productive marine ecosystems, including coral reefs (e.g. Edmunds & Carpenter 2001; Mumby *et al.* 2007), seagrass meadows (reviewed by Valentine & Heck Jr 1999) and kelp forests (reviewed by Filbee-Dexter & Scheibling 2014). In addition, sea urchins form the basis of important nearshore fisheries in many regions of the world (e.g. Andrew *et al.* 2003; Kato & Schroeter 1985). As a result, climate-driven changes in sea urchin populations have the potential to profoundly affect both marine ecosystems and associated fisheries. Much of the ecological research on sea urchins has focused on the roles of predation

and disease in controlling adult abundance and their cascading influence on community structure (e.g. Burt *et al.* 2018; Estes & Duggins 1995; Filbee-Dexter & Scheibling 2014; Lafferty 2004; Mann & Breen 1972). However, despite the widespread recognition of the importance of recruitment variation in controlling population fluctuations in many marine species (Shelton & Mangel 2011), relatively few studies have examined the biotic and abiotic processes controlling the supply of sea urchin larvae, and the degree to which they affect the abundance and dynamics of older life stages.

Changes in climate can affect spatial and temporal patterns of larval supply by influencing the production of larvae by benthic adults and the survival of larvae in the plankton. Increases in ocean temperature and storm-related disturbances can impact larval production by (1) increasing adult mortality via physical disturbance (Ebeling *et al.* 1985) and the spread of water-borne pathogens (Behrens & Lafferty 2004; Lafferty 2004), and (2) reducing adult fecundity by altering food availability (Foster *et al.* 2015; Okamoto 2014) and inhibiting gametogenesis (Basch & Tegner 2007; Cochran & Engelmann 1975). Because sea urchins produce feeding larvae that spend weeks to months in the plankton, increases in ocean temperature can also affect larval development, growth and survival, either directly, or indirectly by altering the availability of their phytoplankton food source (Bertram & Strathmann 1998; Byrne *et al.* 2009; Hoegh-Guldberg & Pearse 1995; Meyer *et al.* 2007; Strathmann 1987). Finally, climate related changes in patterns of ocean circulation can affect the transport of larvae from source to destination (Siegel *et al.* 2008; but see Morgan 2014). Thus, the effects of climatic change on sea urchin recruitment represent cumulative impacts on adult abundance and reproduction, current patterns that transport larvae, and larval development and survival. Because patterns of ocean temperature, circulation and upwelling can vary dramatically in space, the effects of climate change on sea urchin recruitment potentially vary over large spatial scales. A dearth of long-term, high frequency, spatially extensive data has prevented characterizing temporal and spatial variability in larval recruitment in sea urchins, the degree to which it is explained by different sources of environmental variation, and the relative importance of these drivers in accounting for fluctuations in population size.

Here we used a unique 27-year weekly to biweekly time series of newly metamorphosed larvae (which we refer to as “larval recruits”), collected on artificial substrates placed at seven locations distributed across >1000 km of coast in California to: (1) quantify variation in larval recruitment across different temporal and spatial scales; (2) evaluate whether larval recruitment on artificial substrates predicts year-class strength in natural populations; and (3) determine the relative importance of factors contributing to the observed variation in larval recruitment, namely those that affect reproductive output (such as benthic adult abundance and per-capita fecundity)

and oceanographic conditions that affect planktonic larval survival and transport. Due to the correlative nature of our analyses our primary aim was to reveal potential causal relationships that merit further evaluation as drivers of sea urchin recruitment dynamics at spatial and temporal scales relevant to natural populations.

Study system

Populations of the purple sea urchin (*Strongylocentrotus purpuratus*) occupy shallow subtidal and intertidal rocky substrata from at least 27°N on the western coast of the Baja Peninsula (Olivares-Bañuelos *et al.* 2008) to at least 59°N on the Kenai Peninsula in Alaska (Field & Walker 2003). Purple urchins are broadcast spawners and the seasonality of their spawning in California is generally thought to be driven by photoperiod and temperature (Cochran & Engelmann 1975; Gonor 1973; Pearse *et al.* 1986). Fertilized zygotes develop into planktonic echinoplutei and are obligate planktivores that consume phytoplankton (Strathmann 1987). After spending several weeks to months in the plankton individuals begin final metamorphosis and settle to the benthos (Strathmann 1978) at a size of ~500 μm in diameter (Okamoto unpublished data). Larval recruitment varies dramatically among locations at both small and large spatial scales (Ebert 2010).

Collection of newly settled urchins along the coast of California, USA (1990-2016)

Recruitment of newly metamorphosed purple sea urchins was sampled in three major regions along the California coast from 1990 through 2016, with a total of 54,588 observations. Sampling regions (from south to north) included two sites in San Diego (Scripps Pier and Ocean Beach Pier), four sites in the Santa Barbara Channel (Anacapa Island, Stearns Wharf, Ellwood Pier and Gaviota Pier) and one site at Fort Bragg (Figure 1). San Diego and the Santa Barbara Channel lie within the Southern California Bight and Fort Bragg is in northern California. At each site, urchins were collected using nylon-bristled scrub brushes (2.5 cm long bristles and a 6 x 9 cm wooden base) suspended 1 to 2 m from the benthos (Ebert *et al.* 1994). The majority of deployments included 4-8 replicate brushes collected weekly at each site from 1990 to 2003, and biweekly thereafter through 2016. Upon collection brushes were transported to the laboratory in plastic bags and rinsed through a 350 μm mesh sieve. Purple urchins were then identified to species, sorted from other organisms, counted and preserved see (Ebert *et al.* 1994) for further details.

We conducted three primary analyses using these data (see Methods for full details): (1) we examined biweekly, seasonal and interannual trends and spatial correlations in *S. purpuratus* larval recruitment using a Bayesian multivariate time series model; (2) we tested whether trends

in larval recruitment corresponded to year-class strength using a generalized linear mixed effects model; and (3) we nested a linear regression into the Bayesian time series model from (1) to evaluate the degree to which various biotic and abiotic factors explained patterns of sea urchin larval recruitment in northern and southern California. In this latter analysis we linked larval recruitment data to long-term data on sea surface temperature, chlorophyll a (larval food), kelp coverage (adult food), regional upwelling indices, regional adult abundance indices and global climate indices.

Results

(1) Estimated Patio-temporal Trends in Purple Urchin Larval Recruitment

Substantial interannual variability in larval recruitment of *S. purpuratus* was observed with years of poor recruitment (e.g. 1995, 1998, 2005, 2016) that were, on average 1-2 orders of magnitude lower than neighboring years (Figure 2, Figure S1). Larval recruitment was highly synchronous among sites within each of the two regions in the Southern California Bight indicated by mean interannual correlations of r = 0.73 and 0.85 for sites within the Santa Barbara Channel and San Diego, respectively (Figure 2b, c). Within the Santa Barbara Channel, pairwise correlations in interannual trends involving Gaviota, Ellwood and Stearns Wharf were higher (r = 0.86 to 0.90) those involving Anacapa (r = 0.46 to 0.71). This resulted in part because different rates of interannual declines from high larval recruitment in 2011 to a common low value in 2016. Anacapa began to decline in 2012 while the other sites, while the declines at the other sites did not begin until 2014 (Figure 2b, Supplementary Figure 1 b-e). While Santa Barbara Channel sites all exhibited a period of strong increases following the low in 2005, San Diego sites remained below average for the remainder of the time series (Figure 2 c, Supplementary Figure 1 f-g). In contrast, interannual trends in recruitment at Fort Bragg were asynchronous with sites in the Santa Barbara Channel (Figure 2a vs. 2b, mean r = -0.23) and uncorrelated to sites in San Diego (Figure 2a vs. 2c; mean r = 0.12).

Larval recruitment in southern California was highly seasonal, with similar patterns among sites (Figure 3, Figure S2). On average 90% of recruitment occurred from March to July with a single peak in late April/early May (Figure 3a). By contrast recruitment at Fort Bragg in northern California extended over a longer period of time (90% occurred, between January and September) and often included two peaks per year (a large consistent peak around July and a smaller peak in February and March of some years; Figure 3a, S3). The seasonal peaks in recruitment in southern California coincided with the peaks in sea surface chlorophyll (Figure 3a vs. 3b) and troughs in sea surface temperature (Figure 3a vs. 3c). In northern California the primary peak occurred slightly after the peak in chlorophyll a.

(2) Relationship Between larval recruitment and subsequent juvenile year-class-strength.

Recruitment of juvenile purple urchins at shallow subtidal reefs in the Santa Barbara Channel exhibited a significant, positive correlation with larval recruitment to brushes two years prior (Figure 4, $\chi^2_{df=1}$= 9.48, p = 0.002). Years with high larval recruitment corresponded with a nearly three-fold increase in the mean density of juvenile urchins two summers later.

(3) Relationships with Environmental Conditions

Larval recruitment of purple urchins showed strong correlations with local sea surface temperature (SST, Figure 5 a-g, Figure 6 a), and climate indices, specifically ENSO - measured as the multivariate El Niño Southern Oscillation Index (MEI - Figure 5 h-n, Figure 6 f) and the North Pacific Gyre Oscillation (NPGO –Figure 5 o-u, Figure 6 g). The sign of the correlation was opposite between Northern California (Fort Bragg) and Southern California (Santa Barbara Channel and San Diego). The Pacific Decadal Oscillation showed a correlation with larval recruitment only at Fort Bragg (Figure 6 h), but the estimate was highly collinear with that of the MEI leading to inflated variance of both coefficients (Supplemental Figure 3). No correlation was observed between larval recruitment and adult urchin density or canopy kelp (data that were only available for southern California sites; Figure 6 b, e), or the Bakun Upwelling Index (Figure 6c). Sea surface chlorophyll showed no correlation with larval recruitment at Fort Bragg and in the Santa Barbara Channel and a negative correlation in San Diego – the opposite of the hypothesized relationship that more food in the plankton would lead to higher abundances of larvae and higher numbers of larval recruits (Figure 6 d). The network of correlations among these variables are depicted in (Supplemental Figure 4).

In southern California recruitment was orders of magnitude lower during warm, El Niño conditions and during the negative phase of the NPGO with the more southern sites in San Diego responding more strongly to temperature than those further north in the Santa Barbara Channel (Figure 6 a). In contrast, Fort Bragg, the northern California site, responded positively to warmer El Niño conditions and negatively to the NPGO. Importantly, sites in southern California showed opposite relationships from those at Fort Bragg in northern California (Figure 6 f, g). [Note that we fit models with local variables (SST, adults, kelp coverage, chlorophyll, and Bakun upwelling index) and ocean-scale indices (ENSO/NPGO/PDO) separately because of strong functional dependence of the latter with SST]. The correlations between recruitment and both SST and ENSO occurred on roughly 3-5 year cycles, while the correlation with NGPO occurred on decadal scales.

Discussion

Climate change poses significant threats to marine ecosystems. Yet determining how many species and communities will respond to shifting temperature and ocean storm regimes remains a

difficult task. Using a multi-decadal, high frequency, spatially extensive time series we show how large-scale climatic variation can give rise to geographically different responses in larval sea urchin recruitment that were synchronous within regions and asynchronous between them. Larval recruitment of purple sea urchins varied by orders of magnitude among years and responded oppositely to climate in northern versus southern California. Our finding that larval recruitment was a significant factor in determining year class strength in natural populations indicates that large fluctuations in larval recruitment of this prominent herbivore could have far reaching ecological impacts that resonate throughout the regional marine ecosystems (Pearse 2006).

Climate related changes in the supply of sea urchin larvae are thought to be a primary factor contributing to increases in sea urchin populations that have caused the dramatic transformation of benthic communities (Fabricius *et al.* 2010; Hernández *et al.* 2010; Ling *et al.* 2008). Yet until now, no long-term data have corroborated whether urchin larval supply, regulated by climate, can alter year class strength. Demonstrating this link has historically proved challenging because "larval recruitment" can be attenuated by early post-settlement mortality (Connell 1985; Rowley 1989). Our analysis indicates that the year class strength of purple sea urchins in a region is significantly influenced by larval supply. This result points to the possibility that future oceanographic changes may reduce purple urchin recruitment in southern California, but increase it in northern California with potentially cascading effects on benthic ecosystems. The fact that our study shows similar correlations between oceanographic factors and recruitment over a 27-year period, which included multiple ENSO events, suggests that such climatic associations will continue.

While many recruitment-environment correlations break down over time (Myers 1998), our study shows a strong association between urchin larval recruitment and climate over a nearly 3 decade time scale. Although sea urchin larval recruitment data prior to 1990 were not available in the fine temporal scale characterized by our study, there is evidence of ENSO-related recruitment failures in populations in southern California since 1960s. Between 1969 and the early 1980's, recruitment of juvenile sea urchins was anomalously low in El Niño years (Ebert 1983; Tegner & Dayton 1991). Between 1969 and 1977, juvenile recruitment was lowest during the three El Niño years of 1970, 1973, and 1977 at False Point, California near San Diego (Ebert 1983; Tegner & Dayton 1991) and at nearby Point Loma, low recruitment followed the 1982-83 El Niño event (Ebert 1983; Tegner & Dayton 1991). How patterns of larval recruitment may change in the future depends largely on the process underlying their associations with El Niño.

Although climate related changes to both the benthic and planktonic stages of purple sea urchins can affect larval recruitment via their effects on the production of larvae, our analysis shows no significant correlations between larval recruitment and adult abundance, adult food (kelp) or larval food (phytoplankton) – (Figure 6 and Supplemental Figure 3). This narrows down the range to two plausible hypotheses to the regionally varying effects of ENSO and temperature on larval supply and recruitment: (1) temperature-related effects on larval production and survival, and 2) ENSO-related changes in currents that vary between southern and northern California, which affect larval delivery. While adult purple urchins can tolerate temperatures up to 25°C (Farmanfarmaian & Giese 1963), temperatures above 17°C during ENSO events in southern California may adversely affect larval supply via effects on gamete production (Basch & Tegner 2007; Cochran & Engelmann 1975), fertilization (Schroeder & Battaglia 1985) larval development and gene expression (Padilla-Gamiño *et al.* 2013; Runcie *et al.* 2012; Wong *et al.* 2018), and larval survival (Azad *et al.* 2012). Such responses to high temperatures may, in part, explain why recruitment at Fort Bragg, where sea surface temperatures are rarely above 16°C, was not negatively correlated with temperature.

Like variation in temperature, regional circulation is hypothesized to be an important driver of larval recruitment for many species, including those in the Southern California Bight (Blanchette *et al.* 2006; Broitman *et al.* 2005; McManus & Woodson 2012; Woodson *et al.* 2012). ENSO can cause major changes in patterns of ocean circulation along the US west coast, with warm El Niño years often characterized by anomalously strong poleward flow and decreased local retention (Lynn & Bograd 2002; Mitarai *et al.* 2009). Importantly, these effects differ between northern and southern California and may partly explain the divergences in climatic responses in recruitment between these two regions. In northern California, El Niño events are associated with relaxed upwelling and downwelling Kelvin waves (Chavez *et al.* 2002) which hypothetically improves larval retention, but is thought to have a more nuanced impact in the Southern California Bight (Lynn & Bograd 2002; Mitarai *et al.* 2009). Although we cannot definitively partition out the effects of climate associated changes in current patterns and temperature on larval recruitment, our observations on larval recruitment and subsequent year-class strength point strongly to broader-scale ocean climate effects.

Our study demonstrates a consistent and geographically variable relationship between climate and larval recruitment and year-class strength of purple sea urchins over a three-decade time period. These unique time series provide an unprecedented illustration of climate related impacts on larval recruitment dynamics that are notoriously difficult to investigate. We show that fluctuations in larval recruitment can influence year-class strength in an herbivore that is known to severely alter the composition of an entire benthic ecosystem. Although these results

are based on correlations, they were observed consistently over three decades (with further anecdotal evidence spanning six decades) that have included multiple ENSO events. Moreover, our findings provide important insights into the environmental drivers of larval recruitment, which is essential for understanding and predicting the influence of climate on regional population and community dynamics of marine species. Oceans are experiencing simultaneous shifts in temperature, water chemistry, productivity and circulation; thus future investigations aimed at determining the specific biotic and abiotic processes that regulate larval recruitment should provide much needed knowledge of how climate change is influencing regional population dynamics to alter the dynamics and structure marine ecosystems.

Methods

(1) Estimated patio-temporal Trends in Purple Urchin Larval Recruitment

We estimated annual, seasonal, and spatial trends in larval recruitment using an integrated spatio-temporal model that accounted for both the intercorrelated and heterogeneous nature of the multivariate time series. Specifically, we used a Bayesian hierarchical model with spatiotemporal correlations in the underlying annual and seasonal scale trends, and spatial correlations in the process error terms. We used this model to simultaneously estimate biweekly, seasonal and interannual trends in recruitment, and spatial synchrony while accounting for observation noise.

Using this model, we calculated the log-scale biweekly mean trend in larval recruitment as the sum of the estimated annual trend, seasonal trend and process error in the statistical model. The annual trend was estimated using a separable spatio-temporal covariance prior where the spatial covariance is unstructured (i.e. each element estimated) and the temporal covariance determined by a Matérn 3/2 prior. Functionally, we constructed the covariance matrix for the annual trend using Kronecker matrix-vector operations with the Cholesky decompositions of the spatial and temporal correlation functions independently for efficiency (Steeb & Hardy 2011). The seasonal trend within each site was estimated using a periodic temporal covariance (MacKay 1998). The process error (deviations from the sum of smoothed annual and seasonal trends) was modeled with an unstructured spatial covariance, assuming temporal independence. We used a Poisson likelihood to link the expectation (biweekly mean trend) to the observed counts of *S. purpuratus* larval recruits.

Occasionally we encountered samples with sufficiently large numbers of larval recruits (hundreds to thousands of urchins per sample - 1,070 out of 53,478 samples or ~2%), which prevented efficient identification of all urchins to species. In these cases, *S. purpuratus* were

identified from a homogenized subsample of 30-100 individuals. We accounted for the uncertainty in *S. purpuratus* abundance introduced by this subsampling routine by using a beta prior with parameters determined by the subsampled *S. purpuratus* counts and the non-*S. purpuratus* counts. This prior was derived as the analytical posterior distribution of the proportion of the true, latent fraction that was *S. purpuratus* given a Jeffrey's prior on a binomial model of the observed counts.

All equations for the model are given in Supplementary Table 1 and parameters and variables defined in Supplementary Table 2. We estimated the models using Stan (Carpenter *et al.* 2016; Hoffman & Gelman 2014; Stan Development Team 2016b, a) via R (R Core Team 2017) with three 1000 iteration chains after 1000 iteration burn-in. Stan code for the model is provided in the appendix.

(2) Relationship Between larval recruitment and subsequent juvenile year-class-strength.

We tested whether the mean of our estimates of larval recruitment in the Santa Barbara Channel (mean of Anacapa, Stearns Wharf, Ellwood Pier and Gaviota Pier) was predictive of subsequent juvenile recruitment on natural reefs in the region. We calculated juvenile densities from the Channel Islands Kelp Forest Monitoring (KFM) Program (Kushner *et al.* 2013), including only sites whose time series extend from 1990 through 2016. To test for correlations, we used a Bayesian generalized linear mixed effects model (GLMM) with a negative binomial likelihood and survey site as a random effect.

The KFM program surveys purple sea urchins at the Santa Barbara Channel Islands by counting the total number of individuals in defined areas and measuring approximately 100 individuals at each site. Thus, to model density we used the number of juveniles measured divided by the total number of individuals measured, multiplied by the total number of individuals counted, divided by the area surveyed.

$$Juvenile\ Density_{i,t} = \frac{Juveniles\ Measured_{i,t}}{Total\ Meas_{i,t}} \frac{Total\ Count_{i,t}}{Total\ Area_{i,t}}$$

We modeled density in the GLM using the number of measured juvenile urchins (2.5 cm in test diameter- the approximate cutoff size for reproduction; ref Kenner & Lares 1991). Let $\mu_{i,t}$ represent expected juvenile density at site *i* in year *t*. We constructed the regression as:

$$\ln \mu_{i,t} = \alpha_i + \beta \ln Larval\ recruitment_t$$

We allowed the intercept (α_i) to vary by site nested within each island because of overall differences in mean juvenile density among sites and islands. We used a negative binomial (NB) with the using direct mean and variance parameterization form:

$$Juveniles\ Measured_{i,t} \sim \mathrm{NB}\left(\ln \mu_{i,t} - \ln\left[\frac{1}{Tot.Measured_{i,t}} \frac{Tot.Count_{i,t}}{Tot.Area_{i,t}}\right], \sigma^2\right)$$

We constructed the model in this format (i.e. with the density denominator in the left hand side of the equation) to maintain the sample size and integer nature of the data while modeling the mean density. We tested the hypothesis of no correlation using a likelihood ratio test. Models were estimated using glmmTMB (Magnusson *et al.* 2017) in R.

(3) Relationships with Environmental Conditions

We tested how larval recruitment trends correlated with physical and biological variables using two core analyses. Covariates included the following:

(i) Oceanographic climate indices (monthly, 1990-2016, all sites): We used three major global indices of oceanographic climate. The multivariate El Niño Southern Oscillation Index (MEI) provides a metric of the intensity of El Niño/La Niña fluctuations and is derived from several metrics of sea surface temperature, surface winds, sea level pressure, and cloudiness of the sky (Wolter & Timlin 1993; Wolter & Timlin 1998). The Pacific Decadal Oscillation (PDO) is the 1st empirical orthogonal function analysis mode of sea surface temperature variability and height in the Northeast Pacific (Mantua & Hare 2002) and the North Pacific Gyre Oscillation (NPGO) is the 2nd mode (Di Lorenzo *et al.* 2008).

(ii) Coastal upwelling index (monthly, 1997-2016, all sites): The Bakun index (Bakun 1973) provides an index of coastal upwelling and specifically describes the volume of water that is transported offshore from Ekman transport (http://www.pfel.noaa.gov/). Negative values indicate downwelling and surface waters that moved onshore, while positive values indicate upwelling and surface waters moving offshore. This index has been used in relation to delivery of larvae onshore and advection from shore in addition to its value as a metric of coastal productivity. For the Southern California Bight sites, we used data from 33N-119W, while in Northern California we used data from 39N-125W.

(iii) Sea surface chlorophyll (monthly, 1997-2016, all sites): Satellite imagery of sea surface chlorophyll provides a spatially and temporally resolved estimate of phytoplankton biomass that is not available from in situ sampling. Thus, as a metric of planktonic food availability we used version 3.1 of the OC-CCI merged ocean color time series (Sathyendranath *et al.* 2018) from SeaWIFs (O'Reilly *et al.* 1998), MERIS (Rast *et al.* 1999), MODIS (Esaias *et al.* 1998) and VIIRS (Schueler *et al.* 2002) that allows for the temporal and spatial coverage required for this study. Because sea surface chlorophyll concentration data are spatial grids of time series, we

included averaged cells meeting particular geographic conditions for each site. For mainland sites, all cells had to lay within 10 km offshore of the mainland coastline that stretched 150 km in coastline length from the larval recruitment collection site or within 5 km of any island coastline of any island within a 150 km radius. For the site at Anacapa Island, we included any point within a 150 km radius and within 10 km of any coastline. We used 150 km because that is the average Lagrangian estimate for dispersal distances for species with a planktonic larval duration (PLD) of 30-days (Siegel *et al.* 2003). However, this is potentially an overestimate for a 30-day PLD as behavior and complex current patterns may reduce this distance substantially (Shanks 2009). Figure 1 depicts the aerial extent of chlorophyll data used in the analysis.

(*iv) Sea surface temperature (monthly, 1997-2016, all sites):* We used sea surface temperature data derived from Pathfinder AVHRR (advanced very high resolution radiometer) that were optimally interpolated on daily and 0.25 degree latitude/longitude resolution (Reynolds *et al.* 2007). To produce monthly scale time series, we ran data through a 30-day moving average filter with a rectangular, backwards looking window in order to capture general temporal trends in the data. We spatially aggregated data using the same buffers as for chlorophyll indices. Figure 1 illustrates mean spatial trend in winter sea surface temperature for the entire study region.

(v) Fall kelp canopy biomass (annual, 1996-2015, Santa Barbara Channel & San Diego only): The regional biomass of giant kelp *Macrocystis pyrifera* can fluctuate dramatically from year to year (Bell et al. 2015). Giant kelp is a preferred food and a major constituent of *S. purpuratus* diets in southern California (Foster *et al.* 2015). Given that fecundity in *S. purpuratus* can vary by orders of magnitude as a result of food supply (Okamoto 2014), these fluctuations in *M. pyrifera* may in part influence urchin reproduction. Thus, biomass of *M. pyrifera* was derived from Landsat Thematic Mapper satellite imagery (Bell 2017). Data were aggregated for the Santa Barbara Channel (including islands and mainland from Point Conception to Santa Monica Bay through Ventura County) or the San Diego region (mainland coast from the US-Mexico through Orange County including Santa Catalina and San Clemente Islands). We used the 3-month running mean of kelp biomass during the period leading into the spawning season (Sept-Nov) because marked declines in reproductive capacity require several months of consistently low food supply (Okamoto 2014).

(vi) Adult density in the Channel Islands (annual, 1997-2016, Santa Barbara Channel only): As an index of regional adult reproductive density of sea urchins in the Santa Barbara Channel, we used the geometric mean of adult biomass density using survey data from The Channel Islands KFM Program (Kushner et al. 2013). We used the same sites and data as described above (see relationship between urchin larval recruitment and benthic juvenile recruitment) with the exception that instead of juvenile density we used adult biomass density. This was calculated as the biomass of adults based on: (1) the mean relationship between size and individual

12

biomass, (2) the size frequency of adults at a given site in a given year, (3) the total number of urchins, and 4) the total area surveyed.

$$\text{Adult Biomass Density}_t = \frac{1}{S}\sum_{i=1}^{S}\left[\frac{\text{Adults Measured}_{i,t}}{\text{Tot Measured}_{i,t}}\,\frac{\text{Tot Count}_{i,t}}{\text{Tot Area}_{i,t}}\,\frac{1}{N_{i,t}}\sum_{k=1}^{N_{i,t}} f(\text{size}_{k,i,t})\right]$$

To assess which variables exhibited correlations with larval recruitment of purple sea urchins, we nested multiple regression analyses within a time-series modeling framework, where coefficients varied among major regions (Fort Bragg, Santa Barbara, and San Diego sites). The regression analyses included either all global covariates (ENSO, PDO, NPGO) or all local covariates (temperature, chlorophyll, adult densities, kelp coverage, and the Bakun upwelling index). We inserted a centered and standardized regression covariate matrix into the time series model of sea urchin recruitment, replacing the explicit estimates of the interannual trends (Supplementary Table 1). The regression coefficients were given a regularized horseshoe prior (Carvalho *et al.* 2010; Piironen & Vehtari 2017) that biases the model coefficients towards zero without affecting coefficients of relevant variables.

Acknowledgements

Funding was provided by the California Urchin Commission, the South Bay Cable Committee, the California Department of Fish and Game Director's Sea Urchin Advisory Committee, and the National Science Foundation's support of the Santa Barbara Coastal Long Term Ecological Research program. We are indebted to Tom Ebert and John Dixon, who initiated larval recruitment time series with SS. John Richards, Clint Nelson, Shannon Harrer, Jenny Wolf and many students assisted with field collections, laboratory sampling and data compilation. Sally Holbrook, Russ Schmitt and Cherie Briggs contributed discussions during initial development of analyses. Kyle Cavanaugh, Dave Siegel and Tom Bell provided valuable discussions about giant kelp canopy data. Kyle Cavanaugh and Rachel Simons gave important comments on previous manuscript drafts.

13

Figure Captions

Figure 1: Map of larval recruitment collection locations in California. Colors represent the average spatial gradient of sea surface. The hatched white lines show the shoreline buffer used to constrain sea surface temperature and sea surface irradiance (the chlorophyll index) to local larval recruitment observations.

Figure 2: Standardized annual scale trends (log-scale, standardized to one standard deviation) of larval recruitment of purple urchins (*S. purpuratus*) from 1990 through 2016 for: (a) Fort Bragg, (b) sites in the Santa Barbara Channel, and (c) sites in San Diego. Colors within each panel represent individual sites associated with the legend. Interannual trends are estimated using a 3/2 Matérn Gaussian process covariance within a Bayesian multivariate state-space model accounting for spatiotemporal correlations.

Figure 3: Seasonal trends at each site for (a) standardized larval recruitment of *S. purpuratus*, (b) biweekly mean sea surface chlorophyll a (chla) and (c) biweekly mean sea surface temperature (SST). The seasonal trend in larval recruitment at each site was standardized by the mean maximum seasonal value. Chla and SST were measured using satellite imagery within 25 km of the coastline and 150 alongshore km of the location where recruitment was sampled. See Methods for details.

Figure 4: The relationship between the summer density of juvenile purple sea urchins on reefs in the Santa Barbara Channel and the density of recruits on larval collectors during March- July of the previous year (i.e., 12-20 months prior). Points and error bars represent annual means (+/- SE) averaged over all sites. The line with the band represents the estimated relationship and 95% uncertainty interval.

Figure 5: Correlation between purple urchin recruitment at each site and (a-g) sea surface temperature, (h-n) the multivariate ENSO index, and (m-u) the North Pacific Gyre Oscillation (NPGO). Small grey points represent biweekly means and black points and lines represent annual means.

Figure 6: Standardized Bayesian multiple regression coefficients for relationships between *S. purpuratus* and local covariates (a-e) or global climatic indices (f-h). Models with global and local variables were fit separately. Coefficients were estimated using a multiple regression nested within a Bayesian multivariate time series model. Coefficients are a-priori biased towards zero using a horseshoe prior. For details see Methods.

14

Supplementary Tables:

Eq. No	**Description**	**Equation**
Eq. 1	Biweekly estimate	$\hat{\boldsymbol{\mu}} = \exp[\mathbf{X}\beta + \mathbf{Annual} + \mathbf{Seasonal} + \boldsymbol{\varepsilon}]^{\S}$ $\hat{\boldsymbol{\mu}} = \exp[\mathbf{X}\beta + \mathbf{Seasonal} + \boldsymbol{\varepsilon}]^{\ddagger}$
Eq. 2	Subsampling prior	$p_{t,s,b} \sim \text{beta}\left(N_{t,s,b} + 0.5, NO_{t,s,b} + 0.5 \right)$ (if subsampling was performed for brush *b* at time *t* at site *s*)
Eq. 3	Total count likelihood	$N_{t,s,b} \sim \text{Poisson}\left(\hat{\mu}_{t,s} \text{ x } D_{t,s,b}\right)\ if$ sample t, s, b is not subsampled $Tot_{t,s,b} \sim \text{Poisson}\left(\hat{\mu}_{t,s} \times D_{t,s,b}/p_{t,s,b}\right)\ otherwise$
Eq. 4	Prior annual temporal correlation function	$\bar{r}_{sp_{\langle t_i,t_j \rangle}} = \left(1 + 3^2\left\lvert t_i - t_j \right\rvert\right)e^{-3^2\lvert t_i - t_j \rvert}$ (Periodic Kernel - MacKay 1998)
Eq. 5	Prior seasonal temporal correlation function	$\bar{\bar{r}}_{sp_{\langle t_i,t_j \rangle}} = \exp\left[-\frac{2}{1.5^2}\left(0.5 - 0.5\cos\left(\pi\left\lvert t_i - t_j \right\rvert\right)\right)\right]$ (Matérn 3/2 Kernel - Rasmussen & Williams 2006)
Eq. 6[§]	Prior annual spatiotemporal covariance function (separable)	$\bar{\boldsymbol{\Sigma}} = \bar{\boldsymbol{\Omega}} \otimes [\bar{\boldsymbol{\sigma}}\ \bar{\mathbf{R}}]$
Eq. 7	Prior seasonal spatiotemporal covariance function (separable)	$\bar{\bar{\boldsymbol{\Sigma}}} = \bar{\bar{\boldsymbol{\Omega}}} \otimes \left[\bar{\bar{\boldsymbol{\sigma}}}\ \bar{\bar{\mathbf{R}}}\right]$
Eq. 8[§]	Matrix of annual trends	$\mathbf{Annual}_{sp} \sim \text{MVN}(0, \bar{\boldsymbol{\Sigma}})$
Eq. 9	Vector of seasonal trends	$\boldsymbol{Seasonal}_{s,sp} \sim \text{MVN}\left(0, \bar{\bar{\boldsymbol{\Sigma}}}\right)$
Eq. 10	Matrix of process error covariance (spatial)	$\boldsymbol{\varepsilon}_{t,sp} \sim \text{MVN}(0, \sum)$

Supplementary Table 1: Equations for the multivariate spatiotemporal models. Parameters and priors are described in Supplementary Table 2.

[§]only included in the trend estimation model.

[‡]only included in the Bayesian regression model.

15

Symbol	Description	Type	Prior/Input
$\bar{\mathbf{\Omega}}$	Annual scale temporal correlation matrix	Input	Eq. 4
$\bar{\bar{\mathbf{\Omega}}}$	Seasonal scale temporal correlation matrix	Input	Eq. 5
$\bar{\mathbf{R}}$	Annual scale spatial correlation matrix	Estimated (via cholesky factor)	LKJ prior: scale = 2 (Lewandowski *et al.* 2009)
$\bar{\bar{\mathbf{R}}}$	Vector of site-specific annual standard deviations	Estimated	Half-Cauchy: scale = 2.5 (Polson & Scott 2012)
$\bar{\boldsymbol{\sigma}}$	Vector of site-specific seasonal standard deviations	Estimated	Half-Cauchy: scale = 2.5
$\bar{\bar{\boldsymbol{\sigma}}}$	Spatial error covariance matrix	Estimated (via cholesky factor)	LKJ prior[1]: scale = 2
Σ	Site & species specific intercepts and covariate coefficients	Estimated	Intercepts: Student-t: scale= 2 Coefficients: Horseshoe prior (Carvalho *et al.* 2010; Piironen & Vehtari 2017)
$\boldsymbol{\beta}$	Site & species specific first order autoregressive parameter	Estimated	Uniform -0.95 to 0.95
ϕ_s	Total number urchins counted at time *t*, site *s,* on brush *b*	Data	
$N_{t,s,b}$	Number of subsampled urchins at time *t*, site *s,* on brush *b*	Data	
$Tot_{t,s,b}$	Purple urchins counted from the subsample $n_{t,s,b}$	Data	
$NO_{t,s,b}$	Sampling duration of brush *b* at time *t* and site *s*	Data	
X	Covariate Design Matrix	Data	

Supplementary Table 2: Table of parameters and data, descriptions, and priors (if estimated).

References

1. Andrew N., Agatsuma Y., Ballesteros E., Bazhin A., Creaser E., Barnes D., Botsford L., Bradbury A., Campbell A. & Dixon J. (2003) Status and management of world sea urchin fisheries. *Oceanography and Marine Biology-An Annual Review*, 40, 343-425

2. Azad A.K., Pearce C.M. & McKinley R.S. (2012) Influence of stocking density and temperature on early development and survival of the purple sea urchin, *Strongylocentrotus purpuratus* (Stimpson, 1857). *Aquac Res*, 43, 1577-1591

3. Bakun A. 1973. Coastal upwelling indices, west coast of North America, 1946-71. NOAA Tech. Rep. pp. 103.

4. Basch L.V. & Tegner M.J. (2007) Reproductive responses of Purple sea urchin (*Strongylocentrotus purpuratus*) populations to environmental conditions across a coastal depth gradient. *Bull Mar Sci*, 81, 255-282

5. Behrens M.D. & Lafferty K.D. (2004) Effects of marine reserves and urchin disease on southern Californian rocky reef communities. *Mar Ecol Prog Ser*, 279, 129-139

6. Bell T., K. Cavanaugh and D. Siegel, (2017) SBC LTER: Time series of quarterly NetCDF files of kelp biomass in the canopy from Landsat 5, 7 and 8, 1984 - 2016 (ongoing). Santa Barbara Coastal Long Term Ecological Research Project. doi:10.6073/pasta/817d2c24ebd78621869e17d94ba0df0c

7. Bell T.W., Cavanaugh K.C., Reed D.C. & Siegel D.A. (2015) Geographical variability in the controls of giant kelp biomass dynamics. *J Biogeogr*, 42, 2010-2021

8. Bertram D.F. & Strathmann R.R. (1998) Effects of maternal and larval nutrition on growth and form of planktotrophic larvae. *Ecology*, 79, 315-327

9. Blanchette C.A., Broitman B.R. & Gaines S.D. (2006) Intertidal community structure and oceanographic patterns around Santa Cruz Island, CA, USA. *Mar Biol*, 149, 689-701

10. Broitman B.R., Blanchette C.A. & Gaines S.D. (2005) Recruitment of intertidal invertebrates and oceanographic variability at Santa Cruz Island, California. *Limnol Oceanogr*, 50, 1473-1479

11. Burt J.M., Tinker M.T., Okamoto D.K., Demes K.W., Holmes K. & Salomon A.K. (2018) Sudden collapse of a mesopredator reveals its complementary role in mediating rocky reef regime shifts. *Proc R Soc B*, 285

12. Byrne M., Ho M., Selvakumaraswamy P., Nguyen H.D., Dworjanyn S.A. & Davis A.R. (2009) Temperature, but not pH, compromises sea urchin fertilization and early development under near-future climate change scenarios. *Proc R Soc B*, 276, 1883-1888

13. Cai W., Borlace S., Lengaigne M., Van Rensch P., Collins M., Vecchi G., Timmermann A., Santoso A., McPhaden M.J. & Wu L. (2014) Increasing frequency of extreme El Niño events due to greenhouse warming. *Nature climate change*, 4, 111

14. Carpenter B., Gelman A., Hoffman M., Lee D., Goodrich B., Betancourt M., Brubaker M.A., Guo J., Li P. & Riddell A. (2016) Stan: A probabilistic programming language. *J Stat Softw*, 20

17

15. Carvalho C.M., Polson N.G. & Scott J.G. (2010) The horseshoe estimator for sparse signals. *Biometrika*, 97, 465-480

16. Chavez F., Pennington J., Castro C., Ryan J., Michisaki R., Schlining B., Walz P., Buck K., McFadyen A. & Collins C. (2002) Biological and chemical consequences of the 1997–1998 El Niño in central California waters. *Progress in Oceanography*, 54, 205-232

17. Cochran R.C. & Engelmann F. (1975) Environmental regulation of the annual reproductive season of *Strongylocentrotus purpuratus* (Stimpson). *Biol Bull*, 148, 393-401

18. Connell J.H. (1985) The consequences of variation in initial settlement vs. post-settlement mortality in rocky intertidal communities. *J Exp Mar Biol Ecol*, 93, 11-45

19. Di Lorenzo E., Schneider N., Cobb K.M., Franks P., Chhak K., Miller A.J., McWilliams J.C., Bograd S.J., Arango H. & Curchitser E. (2008) North Pacific Gyre Oscillation links ocean climate and ecosystem change. *Geophysical Research Letters*, 35

20. Ebeling A., Laur D. & Rowley R. (1985) Severe storm disturbances and reversal of community structure in a southern California kelp forest. *Mar Biol*, 84, 287-294

21. Ebert T. (1983) Recruitment in echinoderms. *Echinoderm Stud*, 1, 169-203

22. Ebert T., Schroeter S., Dixon J. & Kalvass P. (1994) Settlement patterns of red and purple sea urchins (*Strongylocentrotus franciscanus* and *S. purpuratus*) in California, USA. *Mar Ecol Prog Ser*, 111, 41-52

23. Ebert T.A. (2010) Demographic patterns of the purple sea urchin *Strongylocentrotus purpuratus* along a latitudinal gradient, 1985-1987. *Mar Ecol Prog Ser*, 406, 105-120

24. Edmunds P.J. & Carpenter R.C. (2001) Recovery of Diadema antillarum reduces macroalgal cover and increases abundance of juvenile corals on a Caribbean reef. *Proceedings of the National Academy of Sciences*, 98, 5067-5071

25. Esaias W.E., Abbott M.R., Barton I., Brown O.B., Campbell J.W., Carder K.L., Clark D.K., Evans R.H., Hoge F.E. & Gordon H.R. (1998) An overview of MODIS capabilities for ocean science observations. *IEEE Transactions on Geoscience and Remote Sensing*, 36, 1250-1265

26. Estes J.A. & Duggins D.O. (1995) Sea otters and kelp forests in Alaska: generality and variation in a community ecological paradigm. *Ecol Monogr*, 65, 75-100

27. Fabricius K., Okaji K. & De'Ath G. (2010) Three lines of evidence to link outbreaks of the crown-of-thorns seastar Acanthaster planci to the release of larval food limitation. *Coral Reefs*, 29, 593-605

28. Farmanfarmaian A. & Giese A. (1963) Thermal tolerance and acclimation in the western purple sea urchin, *Strongylocentrotus purpuratus*. *Physiol Zool*, 36, 237-243

29. Field C.M. & Walker C. 2003. *A Site Profile of the Kachemak Bay Research Reserve, a Unit of the National Estuarine Research Reserve System*. Kachemak Bay Research Reserve Homer

30. Filbee-Dexter K. & Scheibling R.E. (2014) Sea urchin barrens as alternative stable states of collapsed kelp ecosystems. *Mar Ecol Prog Ser*, 495, 1-25

31. Foster M.C., Byrnes J.E. & Reed D.C. (2015) Effects of five southern California macroalgal diets on consumption, growth, and gonad weight, in the purple sea urchin *Strongylocentrotus purpuratus*. *PeerJ*, 3, e719

32. Gonor J.J. (1973) Reproductive cycles in oregon populations of the echlnoid, *StrongylocentrotUs purpuratus* (Stimpson). I. Annual gonad growth and ovarian gametogenic cycles. *J Exp Mar Biol Ecol*, 12, 45-64

33. Hernández J.C., Clemente S., Girard D., Pérez-Ruzafa Á. & Brito A. (2010) Effect of temperature on settlement and postsettlement survival in a barrens-forming sea urchin. *Mar Ecol Prog Ser*, 413, 69-80

34. Hoegh-Guldberg O. & Pearse J.S. (1995) Temperature, food availability, and the development of marine invertebrate larvae. *Am Zool*, 35, 415-425

35. Hoffman M.D. & Gelman A. (2014) The No-U-Turn Sampler: Adaptively Setting Path Lengths in Hamiltonian Monte Carlo. *J Mach Learn Res*, 15, 1593-1623

36. Kato S. & Schroeter S.C. (1985) Biology of the red sea urchin, *Strongylocentrotus franciscanus*, and its fishery in California. *Mar. Fish. Rev*, 47, 1-20

37. Kenner M. & Lares M. (1991) Size at first reproduction of the sea urchin *Strongylocentrotus purpuratus* in a central California kelp forest. *Mar Ecol Prog Ser*, 76, 303-306

38. Kushner D.J., Rassweiler A., McLaughlin J.P. & Lafferty K.D. (2013) A multi-decade time series of kelp forest community structure at the California Channel Islands: Ecological Archives E094-245. *Ecology*, 94, 2655-2655

39. Lafferty K.D. (2004) Fishing for lobsters indirectly increases epidemics in sea urchins. *Ecol Appl*, 14, 1566-1573

40. Lewandowski D., Kurowicka D. & Joe H. (2009) Generating random correlation matrices based on vines and extended onion method. *Journal of multivariate analysis*, 100, 1989-2001

41. Ling S.D., Johnson C., Frusher S. & King C. (2008) Reproductive potential of a marine ecosystem engineer at the edge of a newly expanded range. *Global Change Biology*, 14, 907-915

42. Lynn R. & Bograd S. (2002) Dynamic evolution of the 1997–1999 El Niño–La Niña cycle in the southern California Current system. *Progress in Oceanography*, 54, 59-75

43. MacKay D.J. (1998) Introduction to Gaussian processes. *NATO ASI Series F Computer and Systems Sciences*, 168, 133-166

44. Magnusson A., Skaug H.J., Nielsen A., Berg C.W., Kristensen K., Maechler M., Bentham K.J.v., and B.M.B. & Brooks M.E. (2017) glmmTMB: Generalized Linear Mixed Models using Template Model Builder. R package version 0.1.3. Available at https://github.com/glmmTMB

45. Mann K. & Breen P. (1972) The relation between lobster abundance, sea urchins, and kelp beds. *Journal of the Fisheries Board of Canada*, 29, 603-605

46. Mantua N.J. & Hare S.R. (2002) The Pacific decadal oscillation. *Journal of Oceanography*, 58, 35-44

19

47. McManus M.A. & Woodson C.B. (2012) Plankton distribution and ocean dispersal. *J Exp Biol*, 215, 1008-1016

48. Meyer E., Green A., Moore M. & Manahan D. (2007) Food availability and physiological state of sea urchin larvae (*Strongylocentrotus purpuratus*). *Mar Biol*, 152, 179–191

49. Mitarai S., Siegel D., Watson J., Dong C. & McWilliams J. (2009) Quantifying connectivity in the coastal ocean with application to the Southern California Bight. *J Geophys Res*, 114

50. Morgan S.G. (2014) Behaviorally mediated larval transport in upwelling systems. *Advances in Oceanography*, 2014

51. Mumby P.J., Hastings A. & Edwards H.J. (2007) Thresholds and the resilience of Caribbean coral reefs. *Nature*, 450, 98-101

52. Myers R.A. (1998) When do environment–recruitment correlations work? *Rev Fish Biol Fish*, 8, 285-305

53. O'Reilly J.E., Maritorena S., Mitchell B.G., Siegel D.A., Carder K.L., Garver S.A., Kahru M. & McClain C. (1998) Ocean color chlorophyll algorithms for SeaWiFS. *Journal of Geophysical Research: Oceans*, 103, 24937-24953

54. Okamoto D.K. 2014. *The role of fluctuating food supply on recruitment, survival and population dynamics in the sea*. University of California, Santa Barbara

55. Olivares-Bañuelos N.C., Enríquez-Paredes L.M., Ladah L.B. & De La Rosa-Vélez J. (2008) Population structure of purple sea urchin Strongylocentrotus purpuratus along the Baja California peninsula. *Fisheries science*, 74, 804-812

56. Padilla-Gamiño J.L., Kelly M.W., Evans T.G. & Hofmann G.E. (2013) Temperature and CO2 additively regulate physiology, morphology and genomic responses of larval sea urchins, *Strongylocentrotus purpuratus*. *Proc R Soc B*, 280

57. Pearse J.S., Pearse V.B. & Davis K.K. (1986) Photoperiodic Regulation of Gametogenesis and Growth in the Sea Urchin *Strongylocentrotus purpuratus*. *J Exp Zool*, 237, 107-118

58. Pearse J.S. (2006) Ecological role of purple sea urchins. *Science*, 314, 940-941

59. Piironen J. & Vehtari A. (2017) Sparsity information and regularization in the horseshoe and other shrinkage priors. *Electronic Journal of Statistics*, 11, 5018-5051

60. Polson N.G. & Scott J.G. (2012) On the half-Cauchy prior for a global scale parameter. *Bayesian Analysis*, 7, 887-902

61. R Core Team (2017) R: A language and environment for statistical computing. Available at http://www.r-project.org/

62. Rasmussen C.E. & Williams C.K.I. 2006. *Gaussian Processes for Machine Learning*. The MIT Press, Cambridge, Massachusetts

63. Rast M., Bezy J. & Bruzzi S. (1999) The ESA Medium Resolution Imaging Spectrometer MERIS a review of the instrument and its mission. *Int J Remote Sens*, 20, 1681-1702

64. Reynolds R.W., Smith T.M., Liu C., Chelton D.B., Casey K.S. & Schlax M.G. (2007) Daily high-resolution-blended analyses for sea surface temperature. *J Clim*, 20, 5473-5496

65. Rowley R. (1989) Settlement and recruitment of sea urchins (*Strongylocentrotus spp*.) in a sea-urchin barren ground and a kelp bed: are populations regulated by settlement or post-settlement processes? *Mar Biol*, 100, 485-494

66. Runcie D.E., Garfield D.A., Babbitt C.C., Wygoda J.A., Mukherjee S. & Wray G.A. (2012) Genetics of gene expression responses to temperature stress in a sea urchin gene network. *Mol Ecol*, 21, 4547-4562

67. Sathyendranath S., Grant M., Brewin R.J.W., Brockmann C., Brotas V., Chuprin A., Doerffer R., Dowell M., Farman A., Groom S., Jackson T., Krasemann H., Lavender S., Martinez Vicente V., Mazeran C., Mélin F., Moore T.S., Müller D., Platt T., Regner P., Roy S., Steinmetz F., Swinton J., Valente A., Zühlke M., Antoine D., Arnone R., Balch W.M., Barker K., Barlow R., Bélanger S., Berthon J.-F., Beşiktepe Ş., Brando V.E., Canuti E., Chavez F., Claustre H., Crout R., Feldman G., Franz B., Frouin R., García-Soto C., Gibb S.W., Gould R., Hooker S., Kahru M., Klein H., Kratzer S., Loisel H., McKee D., Mitchell B.G., Moisan T., Muller-Karger F., O'Dowd L., Ondrusek M., Poulton A.J., Repecaud M., Smyth T., Sosik H.M., Taberner M., Twardowski M., Voss K., Werdell J., Wernand M. & Zibordi G. (2018) ESA Ocean Colour Climate Change Initiative (Ocean_Colour_cci): Version 3.1 Data. Centre for Environmental Data Analysis

68. Schroeder T. & Battaglia D. (1985) "Spiral asters" and cytoplasmic rotation in sea urchin eggs: induction in *Strongylocentrotus purpuratus* eggs by elevated temperature. *J Cell Biol*, 100, 1056-1062

69. Schueler C.F., Clement J.E., Ardanuy P.E., Welsch C., DeLuccia F. & Swenson H. (2002) NPOESS VIIRS sensor design overview. In: *Earth Observing Systems VI*, pp. 11-24. International Society for Optics and Photonics

70. Shanks A.L. (2009) Pelagic larval duration and dispersal distance revisited. *The Biological Bulletin*, 216, 373-385

71. Shelton A.O. & Mangel M. (2011) Fluctuations of fish populations and the magnifying effects of fishing. *Proceedings of the National Academy of Sciences*, 108, 7075-7080

72. Siegel D., Kinlan B., Gaylord B. & Gaines S. (2003) Lagrangian descriptions of marine larval dispersion. *Mar Ecol Prog Ser*, 260, 83-96

73. Siegel D., Mitarai S., Costello C., Gaines S., Kendall B., Warner R. & Winters K. (2008) The stochastic nature of larval connectivity among nearshore marine populations. *Proceedings of the National Academy of Sciences*, 105, 8974-8979

74. Stan Development Team (2016a) Stan: A C++ library for probability and sampling. Version 2.12.0. . Available at http://mc-stan.org/

75. Stan Development Team (2016b) RStan: the R interface to Stan. Version 2.10.1. . Available at http://mc-stan.org/rstan.html

76. Steeb W.-H. & Hardy Y. 2011. *Matrix Calculus and Kronecker Product: A Practical Approach to Linear and Multilinear Algebra Second Edition*. World Scientific Publishing Company

77. Strathmann M.F. 1987. *Reproduction and development of marine invertebrates of the northern Pacific coast: data and methods for the study of eggs, embryos, and larvae*. Univ. of Wash. Press, Seattle

78. Strathmann R. (1978) Length of pelagic period in echinoderms with feeding larvae from the northeast Pacific. *J Exp Mar Biol Ecol*, 34, 23-27

79. Sydeman W.J., Poloczanska E., Reed T.E. & Thompson S.A. (2015) Climate change and marine vertebrates. *Science*, 350, 772-777

80. Tegner M. & Dayton P. (1991) Sea urchins, El Niños, and the long term stability of Southern California kelp forest communities. *Mar Ecol Prog Ser*, 77, 49-63

81. Valentine J.F. & Heck Jr K. (1999) Seagrass herbivory: evidence for the continued grazing of marine grasses. *Mar Ecol Prog Ser*, 291-302

82. Wolter K. & Timlin M. (1993) Monitoring ENSO in COADS with a seasonally adjusted principal component index. In: *Proc. of the 17th Climate Diagnostics Workshop*, pp. 52-57, NOAA/NMC/CAC, NSSL, Oklahoma Clim. Survey, CIMMS and the School of Meteor., Univ. of Oklahoma, Norman, OK

83. Wolter K. & Timlin M.S. (1998) Measuring the strength of ENSO events: How does 1997/98 rank? *Weather*, 53, 315-324

84. Wong J.M., Johnson K.M., Kelly M.W. & Hofmann G.E. (2018) Transcriptomics reveal transgenerational effects in purple sea urchins exposed to upwelling conditions, and the response of their progeny to differential pCO2 levels. *Mol Ecol*

85. Woodson C.B., McManus M.A., Tyburczy J.A., Barth J.A., Washburn L., Caselle J.E., Carr M.H., Malone D.P., Raimondi P.T., Menge B.A. & Palumbi S.R. (2012) Coastal fronts set recruitment and connectivity patterns across multiple taxa. *Limnol Oceanogr*, 57, 582-596

86. Yeh S.-W., Kug J.-S., Dewitte B., Kwon M.-H., Kirtman B.P. & Jin F.-F. (2009) El Niño in a changing climate. *Nature*, 461, 511

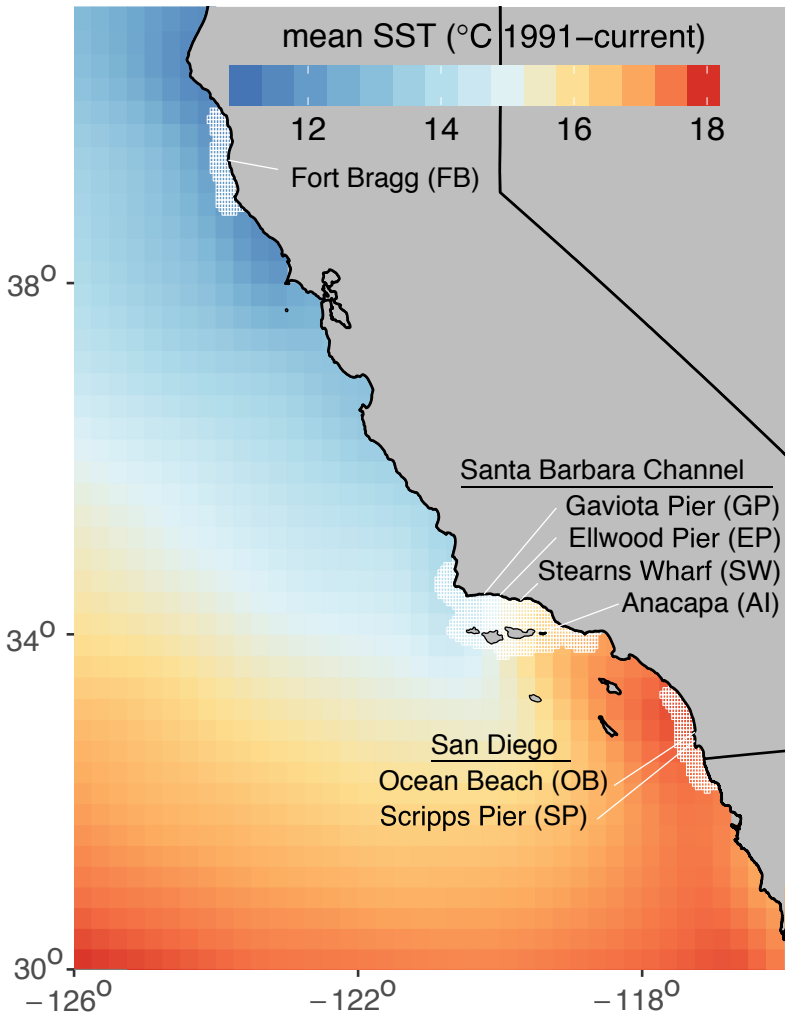
mean SST (°C 1991–current)
12
14
16
18
Fort Bragg (FB)
38°
Santa Barbara Channel
Gaviota Pier (GP)
Ellwood Pier (EP)
Stearns Wharf (SW)
Anacapa (AI)
34°
San Diego
Ocean Beach (OB)
Scripps Pier (SP)
30°
−126°
−122°
−118°

Figure 1

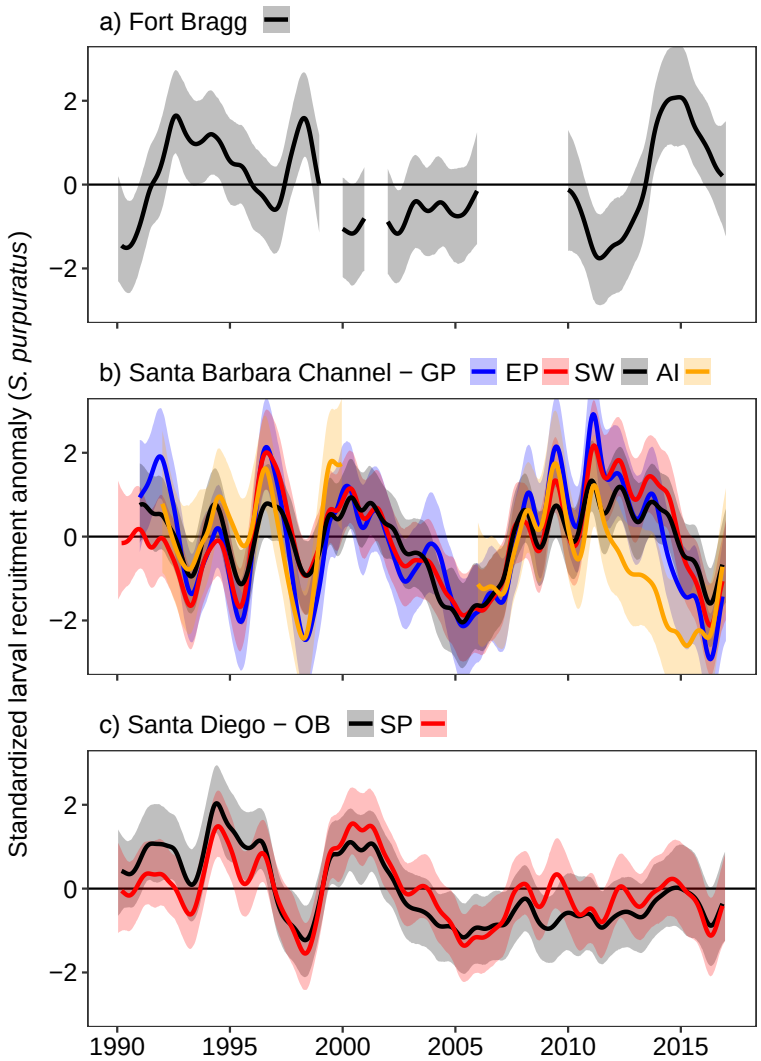
a) Fort Bragg
b) Santa Barbara Channel − GP
EP
SW
AI
c) Santa Diego − OB
SP
Standardized larval recruitment anomaly (S. purpuratus)
2
0
−2
1990
1995
2000
2005
2010
2015

Figure 2

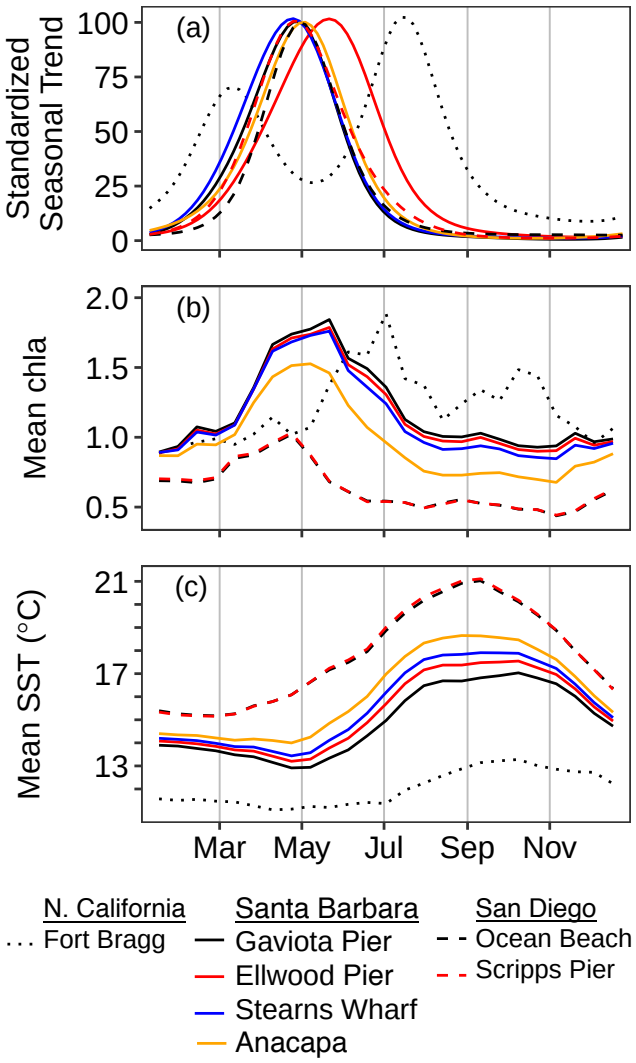
Standardized Seasonal Trend
100
75
50
25
0
(a)
Mean chla
2.0
1.5
1.0
0.5
(b)
Mean SST (°C)
21
17
13
(c)
Mar
May
Jul
Sep
Nov
N. California
Fort Bragg
Santa Barbara
Gaviota Pier
Ellwood Pier
Stearns Wharf
Anacapa
San Diego
Ocean Beach
Scripps Pier

Figure 3

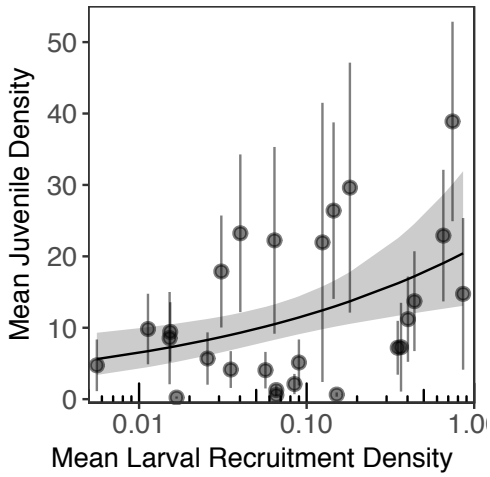
Mean Juvenile Density
50
40
30
20
10
0
0.01
0.10
1.0
Mean Larval Recruitment Density

Figure 4

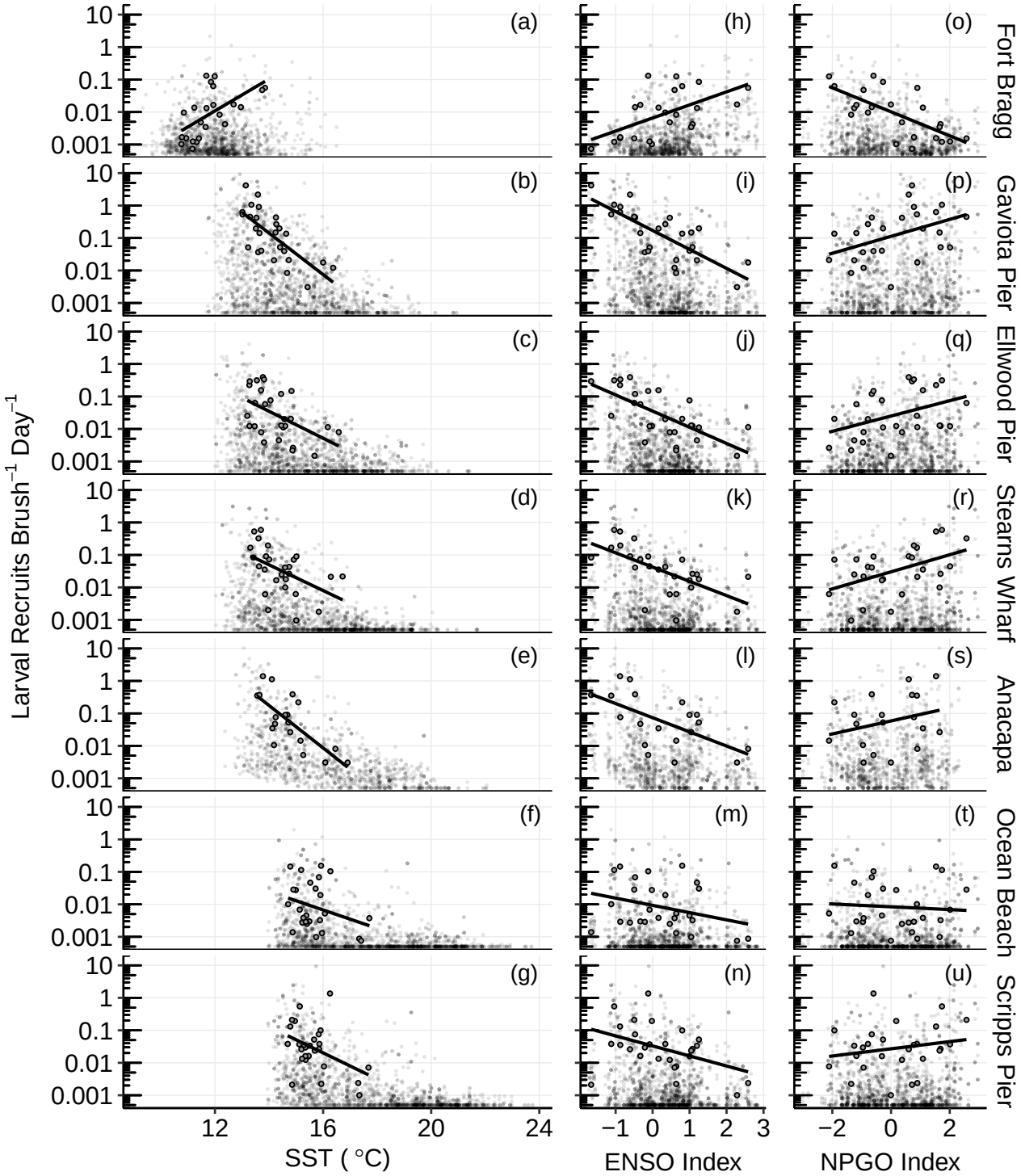
Larval Recruits Brush^{-1} Day^{-1}
10
1
0.1
0.01
0.001
(a)
(b)
(c)
(d)
(e)
(f)
(g)
(h)
(i)
(j)
(k)
(l)
(m)
(n)
(o)
(p)
(q)
(r)
(s)
(t)
(u)
Fort Bragg
Gaviota Pier
Ellwood Pier
Stearns Wharf
Anacapa
Ocean Beach
Scripps Pier
12
16
20
24
SST (°C)
−1
0
1
2
3
ENSO Index
−2
0
2
NPGO Index

Figure 5

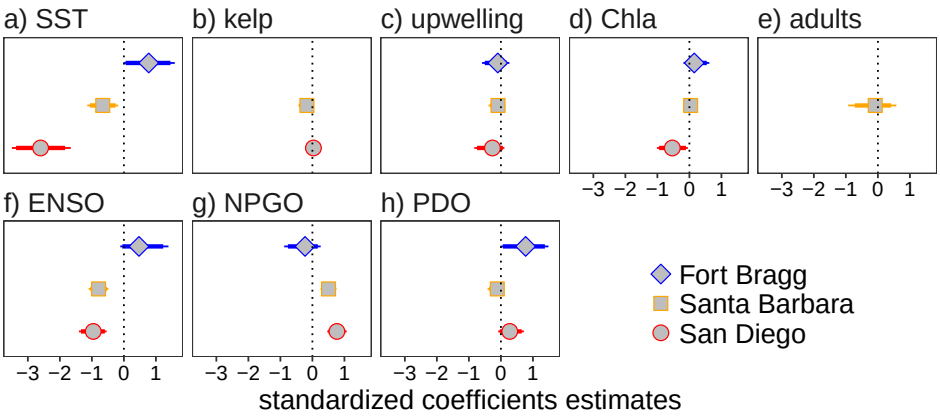
a) SST
b) kelp
c) upwelling
d) Chla
e) adults
f) ENSO
g) NPGO
h) PDO
−3 −2 −1 0 1
Fort Bragg
Santa Barbara
San Diego
standardized coefficients estimates

Figure 6

Supplementary Information - Appendices for "Geographically Opposing Responses of Sea Urchin Recruitment to Changes in Ocean Climate"

Daniel K. Okamoto*[1,2], Daniel C. Reed†[3], and Stephen Schroeter‡[3]

[1]Department of Biological Science, Florida State University, Tallahassee, Florida 32303
[3]Ecology, Evolution and Marine Biology, University of California Santa Barbara, Santa Barbara, CA 93106 USA
[3]Marine Science Institute, University of California Santa Barbara, Santa Barbara, CA 93106 USA

*corresponding author: dokamoto@bio.fsu.edu
†email: dan.reed@lifesci.ucsb.edu
‡email: schroete@lifesci.ucsb.edu
*corresponding author: dokamoto@bio.fsu.edu
†email: dan.reed@lifesci.ucsb.edu
‡email: schroete@lifesci.ucsb.edu

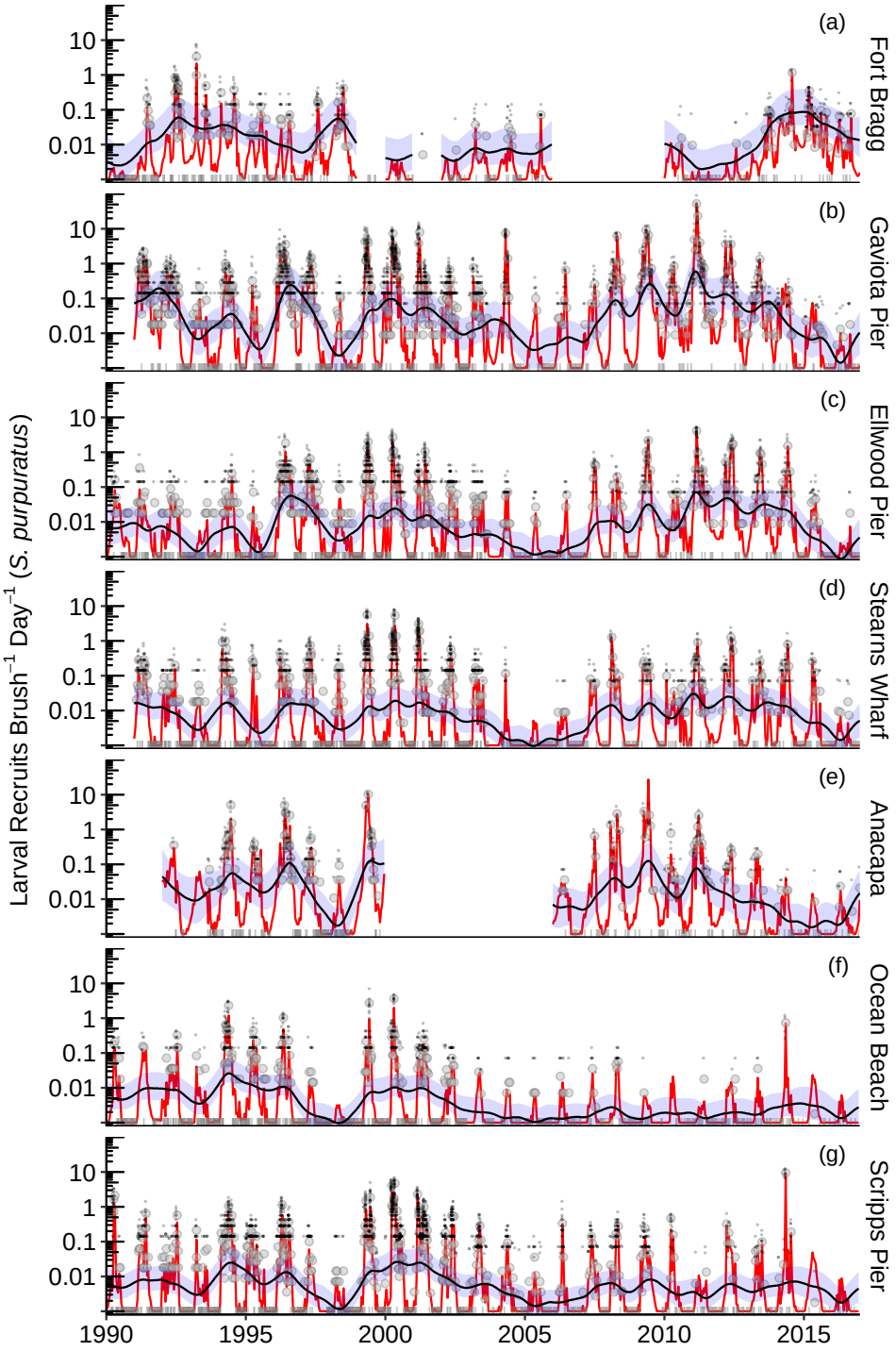

Figure S.1: Observed and estimated purple urchin (*S. purpuratus*) settlement trends from 1990-2016 for each site. Large points represent empirical biweekly means (non-zero means across all brushes and collection times), lines on the axis represent biweekly mean values equal to zero, small points represent counts on individual brushes (non-zero only), red lines represent biweekly estimates, lines with blue 95% uncertainty intervals represent model estimates of the interannual trends. The model estimates the seasonal trend and the interannual trend at each site simultaneously. For reference, interannual trends for *S. purpuratus* shown here are the unstandardized versions of those shown in Figure 2.

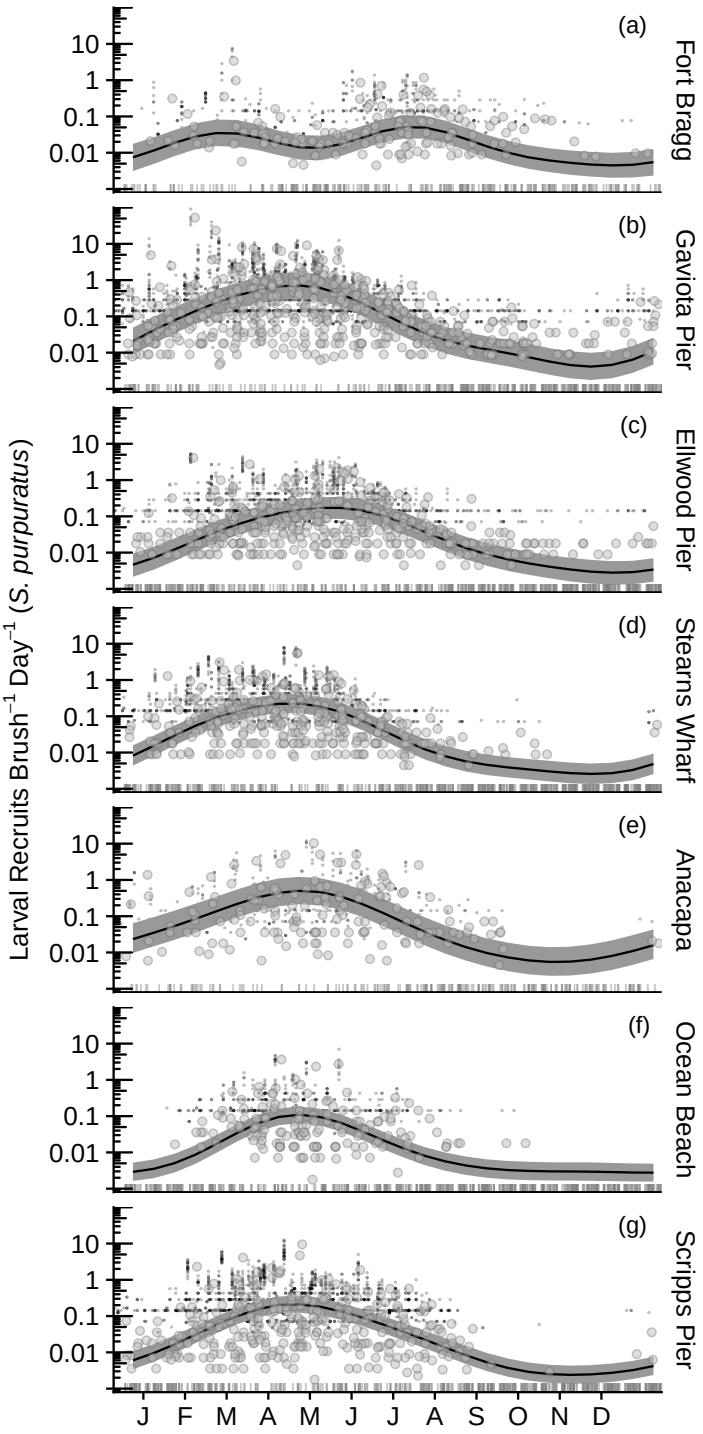

Figure S.2: Seasonal settlement trends from 1990-2016 with the mean estimated seasonal trend for each site. Large points represent empirical biweekly means (non-zero means across all brushes and collection times), lines on the axis represent biweekly mean values equal to zero, small points represent counts on individual brushes (non-zero only), black lines represent the posterior mean and bands represent the 95% uncertainty interval. The model estimates the seasonal trend and the interannual trend at each site simultaneously. For reference, seasonal trends for *S. purpuratus* shown here are the unstandardized versions of those shown in Figure 3.

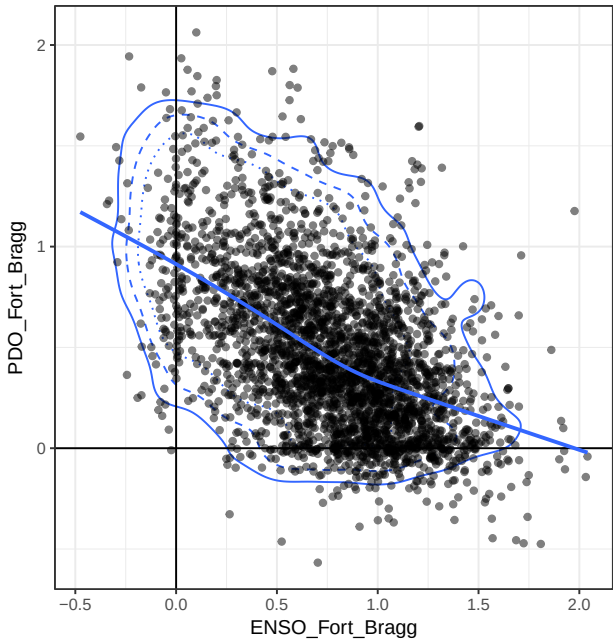

Figure S.3: Correlation between coefficients for ENSO and PDO at Fort Bragg creating variance inflation. Contours represent the 95%, 90% and 80% quantile estimates from 3000 posterior samples. Note that when one is at or near zero, the other is centered away from zero.

Variable Correlations

To illustrate the intercorrelated nature of the covariates and responses, we estimated a network model for Gaviota Pier that includes the independent model estimates of *S. purpuratus* settlement and its seasonality. To do so, we first constrained network structure by excluding all nonsensical interactions (i.e. chlorophyll does not cause ENSO events and is thus eliminated a priori) and including all known directional interactions (i.e. estimated seasonality affecting settlement for is forced into the network). Learning of the network skeleton is achieved via the Hill Climbing algorithm using the bnlearn[1] package in R. Note that strong collinearity can result in the weaker correlation being ignored (e.g. ENSO over SST with Larval Recruitment).

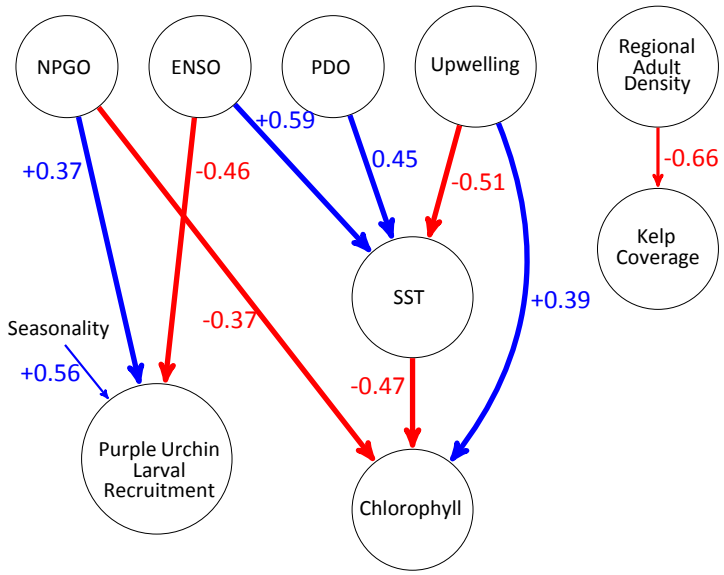

Figure S.4: Bayesian network model structure inferred for the Santa Barbara Channel. Numbers represent the partial correlation coefficients accounting for all other variables pointing to that node. All correlations shown are significant at alpha= 0.05

[1]Marco Scutari (2010). Learning Bayesian Networks with the bnlearn R Package. Journal of Statistical Software, 35(3), 1-22. URL http://www.jstatsoft.org/v35/i03/

```
\\\
```

```
  matrix[NM,NS] e;    // spatially correlated process errors

  LS  = D_seas*z_s;
  w = D_ann*transpose(L_Omega_Spatial*w_z);
  e = transpose(diag_pre_multiply(sigma_S_mu,L_Omega_S)*e_z);

  theta2 = rep_vector(1.0,NO);
  theta2[SUB] = theta;

  // caculate expected values
  S= rep_matrix(mu_S,NM)+diag_post_multiply(LS[PRED_MONTH,],sigma)+
     diag_post_multiply(w,sigma)+e;
  S_exp = exp(to_vector(S)[OBS]) .*D ./theta2;
}

model {
  // site SDs for annual, seasonal trends and process errors
  sigma ~ cauchy(0, 0.5);
  sigma2 ~ cauchy(0, 0.5);
  sigma_S_mu ~ cauchy(0,2.5);

  // spatial correlations for annual and seasonal trends
  L_Omega_S ~ lkj_corr_cholesky(2);
  L_Omega_Spatial ~ lkj_corr_cholesky(2);

  for(i in 1:NS){
    z_s[i]~ normal(0,1);
    mu_S[i] ~ normal(0,5); // site specific log-scale means
  }

  // uncertainty on proportions of purples in the sample
  // jeffrey's prior given subsampling
  theta~beta(P1, P2);

  // observation likelihood
  N ~ poisson( S_exp );
}

generated quantities {
  corr_matrix[NS] Omega_S;
  corr_matrix[NS] Omega_Spatial;
  Omega_S = multiply_lower_tri_self_transpose(L_Omega_S);
  Omega_Spatial = multiply_lower_tri_self_transpose(L_Omega_Spatial);
}
```